Effect of Notch1 on neural tube defects and neural stem cell differentiation induced by all-*trans* retinoic acid

NA CHEN[1,2], JIAMING XU[1], XINYING ZHANG[1], SHUWEI LI[3], WEIWEI ZHU[3], HAIBIN CUI[1], YU SUN[1], BO HAN[1,2] and AIHUA MA[1,2]

[1]Department of Pediatrics, Shandong Provincial Hospital, Cheeloo College of Medicine, Shandong University; [2]Department of Pediatrics, Shandong Provincial Hospital Affiliated to Shandong First Medical University; [3]Department of Pediatrics, Jinan Central Hospital Affiliated to Shandong University, Jinan, Shandong 250021, P.R. China

Received August 18, 2020; Accepted December 18, 2020

DOI: 10.3892/mmr.2021.11859

Abstract. Neural tube defects (NTDs) are the most serious and common birth defects in the clinical setting. The Notch signaling pathway has been implicated in different processes of the embryonic neural stem cells (NSCs) during neural tube development. The aim of the present study was to investigate the expression pattern and function of Notch1 (N1) in all-*trans* retinoic acid (atRA)-induced NTDs and NSC differentiation. A mouse model of brain abnormality was established by administering 28 mg/kg atRA, and then brain development was examined using hematoxylin and eosin (H&E) staining. The N1 expression pattern was detected in the brain of mice embryos via immunohistochemistry and western blotting. NSCs were extracted from the fetal brain of C57 BL/6 embryos at 18.5 days of pregnancy. N1, Nestin, neurofilament (NF), glial fibrillary acidic protein (GFAP) and galactocerebroside (GALC) were identified using immunohistochemistry. Moreover, N1, presenilin 1 (PS1), Nestin, NF, GFAP and GALC were detected via western blotting at different time points in the NSCs with control media or atRA media. H&E staining identified that the embryonic brain treated with atRA was more developed compared with the control group. N1 was downregulated in the embryonic mouse brain between days 11 and 17 in the atRA-treated group compared with the untreated group. The distribution of N1, Nestin, NF, GFAP and GALC was positively detected using immunofluorescence staining. Western blotting results demonstrated that there were significantly, synchronous decreased expression levels of N1 and PS1, but increased expression levels of NF, GFAP and GALC in NSCs treated with atRA compared with those observed in the controls ($P<0.05$). The results suggested that the N1 signaling pathway inhibited brain development and NSC differentiation. Collectively, it was found that atRA promoted mouse embryo brain development and the differentiation of NSCs by inhibiting the N1 pathway.

Correspondence to: Professor Aihua Ma and Professor Bo Han, Department of Pediatrics, Shandong Provincial Hospital, Cheeloo College of Medicine, Shandong University, 324 Jingwu Road, Jinan, Shandong 250021, P.R. China
E-mail: aihuama@hotmail.co.uk
E-mail: hanbo35@163.com

Key words: neural tube defects, brain development, neural stem cells, all-*trans* retinoic acid, Notch1 pathway

Introduction

Neural tube defect (NTD) is a serious congenital defect that occurs during brain development. NTDs are caused by closure anomalies during the development of the neural tube in the embryonic stage, and are mainly manifested in the absence of the brain, brain expansion, meningeal membrane expansion and recessive spinal bifida (1,2). Neural stem cells (NSCs) are key cells involved in nerve tube closure and these cover the surface of nerve tubes (3). NSC proliferation, differentiation and migration serve a pivotal role in the normal closure of nerve tubes, and abnormal differentiation will lead to brain abnormalities (4,5). NSCs are the least committed cells in the nervous system and have self-renewal and pluripotent functional properties, as well as produce all three basic neuroectoderm lineages (6). NSCs produce neurons, astrocytes and oligodendrocytes in a region-appropriate and stage-appropriate manner throughout their lifespan (7).

In various cell fate regulatory pathways, the Notch signal pathway serves a precise and complex regulatory role in cell proliferation and differentiation and in embryonic development (8). The Notch signaling pathway is an evolutionarily conserved mechanism that functions in multiple cell determination processes during metazoan development and in adults (8). The core elements of the vertebrate Notch signaling system include the Notch receptors [Notch 1 (N1)-Notch 4], Delta (Delta l-Delta 4), Serrate/Jagged (Jagged 1-Jagged 2) ligands and the DNA binding protein RBPjk/CBF1 (9). This system allows neighboring cells to communicate with each other via local short-range intercellular interactions, amplifying and consolidating molecular differences which, eventually, manifest as different cell fates. Therefore, disruption of this pathway has functional consequences for multiple different tissues and cell fates (10). The current model for Notch signaling assumes that after ligand binding to the

Notch receptor via its extracellular domain, the intracellular domain of the ligand is ubiquitinated, triggering its endocytosis, which is activated by the action of presenilin γ-secretase enzymes (8).

All-*trans* retinoic acid (atRA) is a normal metabolite of retinoic acid present in the body and is an important factor in embryonic development (11). Previous studies have reported that excess atRA leads to the occurrence of NTDs (12,13). However, its specific molecular mechanism remains to be elucidated.

The present study demonstrated the role of N1 in embryonic brain tissue from mice (*in vivo*) and in NSCs (*in vitro*) treated with atRA. Furthermore, the regulatory effect of N1 on the differentiation of NSCs and the molecular mechanism of brain abnormality caused by atRA treatment were identified. These results may provide a novel direction for the application of NSCs and clinical prevention of brain abnormality.

Materials and methods

Reagents. Anti-N1 (cat. no. ab52627), anti-presenilin1 (PS1; cat. no. ab16244), anti-Nestin (cat. no. ab22035), anti-neurofilament (NF; cat. no. ab204893), anti-glial fibrillary acidic protein (GFAP; cat. no. ab10062), anti-galactocerebroside (GALC; cat. no. ab232972) and anti-β tubulin (cat. no. ab6046) were obtained from Abcam. All other reagents and chemicals were purchased from Sigma-Aldrich (Merck KGaA) unless stated otherwise.

Source of tissue. In total, 24 mice were purchased from the Experimental Animal Center of Shandong University. Mice were housed in conditions at 23±1˚C with a constant humidity of 60±10% under a 12 h light/dark cycle, and had free access to food and water. The research was approved by the Medical Ethics Committee of Shandong Provincial Hospital Affiliated to Shandong First Medical University.

Tissue preparation. Female C57BL/6 mice (age, 10-12 weeks; weight, 25-30 g) were mated with mature males (age, 7-8 weeks; weight, 18-25 g), and the detection of a vaginal plug was designated as embryo day 0 (E0). A total of 24 mice were used. According to a study by Seegmiller *et al* (14), on E7, 12 female mice in the treatment group were administered with all-*trans* atRA (100 mg/kg; Sigma-Aldrich; Merck KGaA) dissolved in corn oil via oral gavage. The other 12 female mice in the control group were administered with the same volume of corn oil. All pregnant mice were sacrificed via cervical dislocation on E11, E13, E15 and E17. The embryos were anesthetized with 10% chloral hydrate (350 mg/kg body weight) via intraperitoneal injection and perfused intracardially with normal saline. No signs of peritonitis, pain or discomfort were observed in the embryos. The mice brains were obtained for hematoxylin and eosin (H&E) staining, as well as immunohistological and western blot analyses.

H&E staining. Embryo brains from atRA-treated and control mice on E11, 13, 15 and 17 were fixed with 4% paraformaldehyde at room temperature for 15 min, snap frozen in liquid nitrogen-cooled isopentane and embedded in Optimal Cutting Temperature, followed by storage at -20˚C. Cryostat sections (thickness, 7 μm) were prepared and immersed in Harris' hematoxylin at 4˚C for 5 min to stain all nuclei. Sections were then washed with cold running tap water for 10 min, counterstained with eosin at 4˚C for 2 min and washed for 10 min with cold running tap water. The sections were visualized and images captured using a Leica (DMRAZ) confocal microscope (magnification, x40; Leica Microsystems, Inc.).

Immunolocalization of N1 in fetal mice. For immunostaining of cryosections, cryostat sections were prepared as aforementioned, and then were fixed for 15 min at room temperature with 4% paraformaldehyde and permeabilized for 15 min in 0.2% Triton X-100. After three washes with PBS, the sections were incubated in room temperature for 2 h with a primary antibody directed against N1 (1:100 in PBS). Following three 10-min washes in PBS, the sections were incubated in room temperature for 2 h with appropriate Alexa Fluor 594 secondary antibodies (1:1,000 in PBS; cat. no. A30008; Molecular Probes; Thermo Fisher Scientific, Inc.). After an additional three washes with PBS, the sections were mounted in Hydromount containing bis-benzimide (Hoechst 33342; 1:500 of 1 mg/ml stock solution; BDH Chemicals Ltd.) to visualize the nuclei. Substitution of the primary antibodies with same species non-immune serum (Abcam) served as the negative controls. The sections were visualized and images captured using a Leica (DMRAZ) microscope (magnification, x40; Leica Microsystems, Inc.) and a fluorescent image analysis software (Quantimet 500; Leica Microsystems, Inc.).

Western blotting for embryonic tissues. Western blot analysis was used to further confirm N1 expression in fetal mice. Total protein was isolated from atRA-treated or control embryonic brain tissues as previously described (15) using RIPA lysis buffer (Thermo Fisher Scientific, Inc.) supplemented with protease and phosphatase inhibitors at 4˚C for 30 min. Proteins were then centrifuged at 15,000 x g at 4˚C for 30 min. Subsequently, 10% SDS-PAGE was used to separate equal amounts (30 μg) of extracted protein samples, which were then transferred to nitrocellulose membranes (EMD Millipore). The membranes were blocked with 5% evaporated skimmed milk at 37˚C for 1 h and incubated with primary antibodies against N1 and β-tubulin (1:1,000) in 5% evaporated skimmed milk at 4˚C for 12 h. Membranes were then incubated with horseradish peroxidase-conjugated secondary antibody (1:2,000; cat. no. 7074s; Cell Signaling Technology, Inc.) in 5% evaporated skimmed milk at 37˚C for 1 h. An ECL kit (Cell Signaling Technology, Inc.) and the ImageQuant Las 4000 mini system (Cytiva) was used to observe the protein bands. β-tubulin was used as an internal control. ImageJ version 1.48 u software (Nationals Institutes of Health) was used to semiquantify the signal intensities.

Isolation and culture of neural stem cells. Embryonic brains were isolated from female mice at E18.5. In brief, 10% chloral hydrate (350 mg/kg body weight) was used as an anesthetic in pregnant mice at E18.5. No signs of peritonitis, pain or discomfort were observed in the embryos. Pregnant mice were sacrificed via cervical dislocation, and fetal mouse brain tissue was removed and placed in a flat dish containing 4% D-Hanks liquid. The brain tissue was cut into 1 mm^3 sections. After

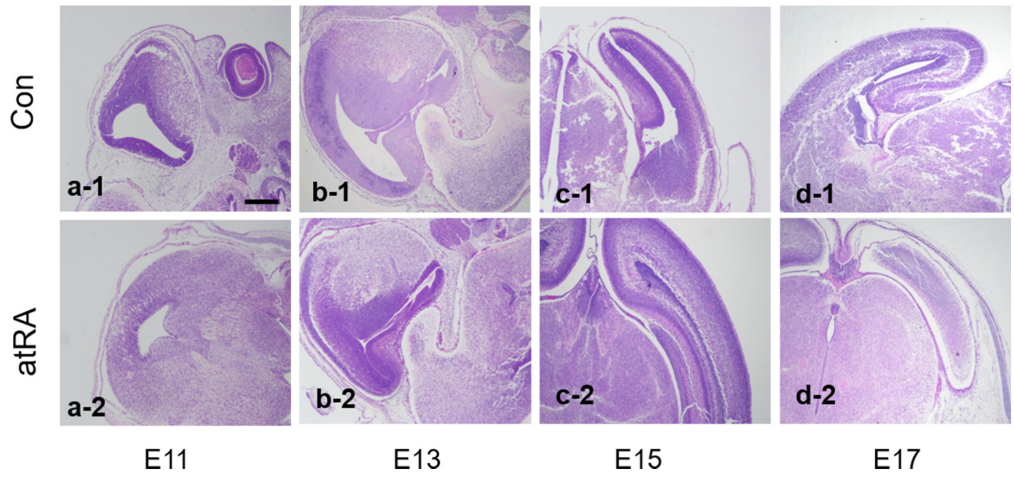

Figure 1. Hematoxylin and eosin staining of embryo mouse brain with control treatment and atRA treatment at different time points. There was a difference in the morphology of the embryonic brain after atRA treatment. a-1-d-1 show the brains isolated from control embryos on E11, 13, 15 and 17. a-2-d-2 are brains isolated from atRA-exposed embryos on E11, 13, 15 and 17. Scale bar, 40 μM. atRA, all-*trans* retinoic acid; E, embryonic day; Con, control.

placing the tissue block in a centrifuge tube, the D-Hanks solution was absorbed and 0.125% trypsin was added at 37˚C and 5% CO_2. The digestion was oscillated for 20 min and then 10% FBS in DMEM (Invitrogen; Thermo Fisher Scientific, Inc.) at 4˚C was used to terminate differentiation for 20 min. DMEM-F12 medium with 20 ng/ml bFGF and 20 ng/ml EGF added to suspend cells, which were cultured in incubators at 37˚C and 5% CO_2. The following day, fresh bFGF and EGF were added. The liquid was changed after 3.5 days, and the culture was passed from days 7-9.

Co-immunolabelling for confirmation. Cultures were fixed with 1% paraformaldehyde at room temperature for 20 min and washed twice with PBS for 5 min. Cells were incubated with 0.2% Triton X-100 (v/v PBS) for 20 min at room temperature to permeabilize the cell membranes, and were then washed twice in PBS (10 min each). The cells were incubated with primary antibodies against N1 with Nestin (N1 + Nestin; 1:100), NF (N1 + NF; 1:100), GFAP (N1 + GFAP; 1:100) and GALC (N1 + GALC; 1:100) for 2 h at room temperature, followed by a 2-h incubation with Alexa Fluor 488 (1:1,000; cat. no. A32723; Molecular Probes; Thermo Fisher Scientific, Inc.) and 594 secondary antibodies (1:1,000; cat. no. A30008; Molecular Probes; Thermo Fisher Scientific, Inc.) at room temperature. After an additional three washes with PBS, the cells were mounted in Hydromount containing bis-benzimide as aforementioned. Substitution of the primary antibodies with same species non-immune serum (Abcam) served as negative controls. The cells were visualized and images were captured using a Leica fluorescent microscope (magnification, x100; Leica Microsystems, Inc.) and a fluorescent image analysis software (Quantimet 500; Leica Microsystems, Inc.).

Western blot analysis for the differentiation of NSCs after treatment with atRA. The 5th-generation nerve spheres were arranged in two groups (experimental and control group) and the medium was discarded after centrifugation in 1,000 x g at room temperature for 10 min. Induced-differentiation media (DMEM with 20 ng/ml bFGF, 20 ng/ml EGF and N2 additives) with or without 1 μmol/l atRA was added at 37˚C to nerve sphere on days 1, 3, 5 and 7. The culture medium was replaced every 24 h for western blotting.

Proteins isolated from atRA-treated or control cultured NSCs were analyzed using western blot analysis, as aforementioned. The primary antibodies used were N1, PS1, NF, GFAP and GALC (1:1,000). β-tubulin (1:1,000) was used as an internal control.

Statistical analysis. The statistically significant differences between groups were analyzed using one-way ANOVA followed with Tukey's multiple comparison test or unpaired Student's t-test, using GraphPad Prism version 4.0 software (GraphPad Software, Inc.). Data are presented as the mean ± SD. All experiments were repeated ≥3 times. $P<0.05$ was considered to indicate a statistically significant difference.

Results

atRA induces brain abnormality in mouse embryos. atRA was administered to female mice on E7. H&E staining identified the morphological changes in the mouse brain of atRA-treated embryos and controls at E11, 13, 15 and 17 (Fig. 1). On E11, the embryos exposed to atRA showed earlier symmetric brain matter formation compared with those in the control group, based on visual observation. On E13, brain matter grew more apparently between atRA-treated and control embryos. On E15, meninges nearly contacted with the opposing side in atRA-exposed embryos, whereas control embryos exhibited uncontacted meninges. On E17, the meninges and brain matter remained unformed and the medial edge epithelium was uncontacted in untreated embryos; however, in atRA-exposed embryos, the two sides of meninges were contacted and the brain matter was already developed.

N1 expression is decreased in mouse brains from atRA-treated embryos. To identify the effects of atRA-induced Notch signaling events on brain development, the expression of N1 in the brains of mice from atRA-treated and untreated E11 and E17 embryos was detected (Fig. 2Aa-1-d-2). The expression of

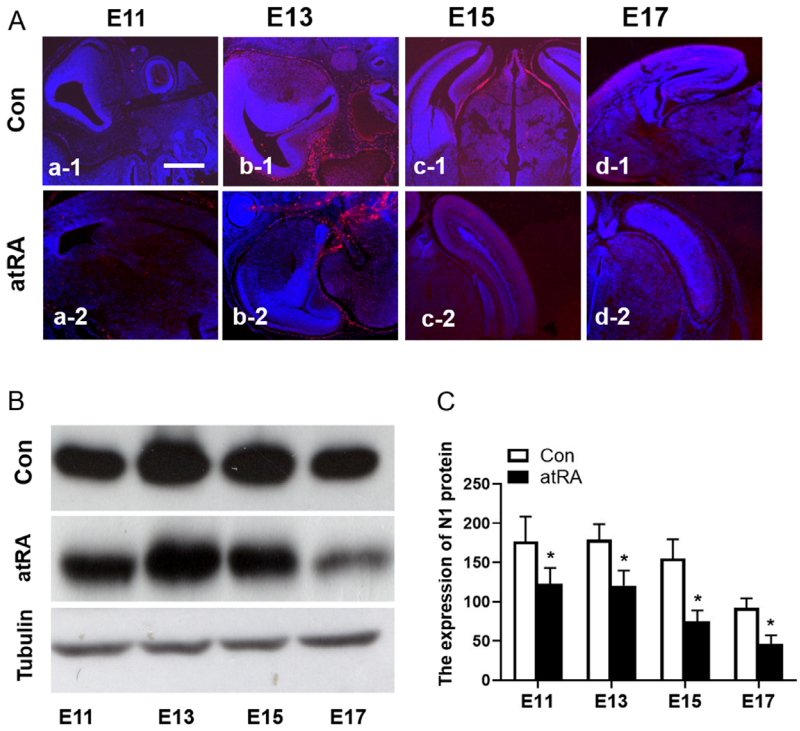

Figure 2. Immunolocalization and the expression of N1 from embryo mouse brain. (A-a-1-d-1) N1 was immunolocalized on local epithelial layers in control media (Con, red). (A-a-2-d-2) N1 appeared to express on epithelium but it seems less appearance in atRA media than control media (red). Blue indicates Hoechst-labelled nuclei. Scale bar, 40 μM. Immunohistochemistry revealed the expression of N1 in palatal tissue isolated from control and atRA-treated embryos between E11 and E17. (B) Expression of N1 in E11, 13, 15 and 17 mice brains with the control media (Con) or atRA media as detected via western blotting. Tubulin was used as a control. (C) Semiquantification of results of N1 expression in mice brains isolated from atRA-exposed and control E11-17 embryos. *P<0.05 vs. Con group. atRA, all-*trans* retinoic acid; E, embryonic day; Con, control; N1, Notch1.

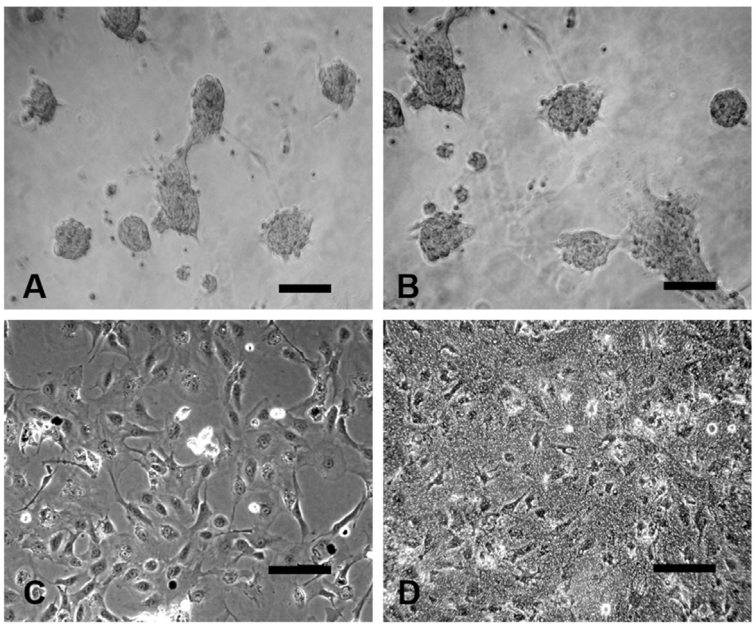

Figure 3. Primary NSC culture and differentiation. (A) Primary NSC culture on day 0, showing a plurality of neurospheres formed. (B) Then, 1 day after differentiation, the shape of neurospheres began to change, and some NSCs were released from the neurospheres. (C) A total of 3 days after differentiation, the number of neurospheres appears to decrease, extending cord-like projection. (D) After 7 days, numerous differentiated forms of nerve cells were observed. Scale bar, 40 μm. NSC, neural stem cell.

N1 was further confirmed via western blotting (Fig. 2B), the expression of N1 was significantly downregulated in embryos treated with atRA compared with the control group (Fig. 2C; Table I; P<0.05).

NSC culture shows differentiated neural cells. The cells that grew in the culture medium continued to undergo morphological changes. Primary NSC culture on day 0 (Fig. 3A) show a plurality of formed neurospheres, which were attached on

Table I. Data of Notch1 expression of mice brain on E11, 13, 15 and 17 with the control media (-atRA) or atRA media (+atRA) from western blotting.

	Control			+atRA			
Day	Exp.1	Exp.2	Exp.3	Exp.1	Exp.2	Exp.3	P-value
E11	131.40	106.80	88.70	42.30	81.30	53.90	0.032
E13	192.10	175.60	136.20	123.20	111.30	79.50	0.0058
E15	116.20	101.30	88.60	65.90	37.50	63.70	0.049
E17	92.20	78.30	82.50	41.60	59.20	11.80	0.047

Control, without all-*trans* retinoic acid; +atRA, with all-*trans* retinoic acid; E, embryonic day; Exp., experiment.

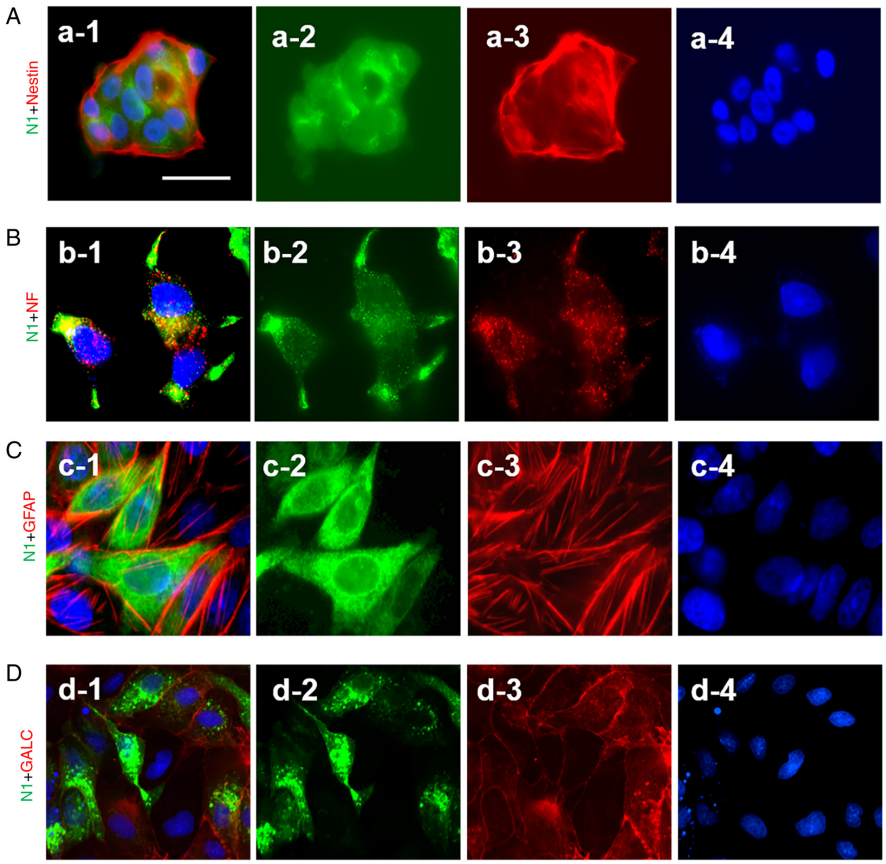

Figure 4. Co-immunostaining detected the expression of N1 with Nestin, NF, GFAP and GALC in neurons, astrocytes and oligodendrocytes, respectively. (A-a-1-a-4) Staining of N1 + Nestin, N1, Nestin and NSC nuclei respectively. (B-b-1-b-4) Staining of N1 + NF, N1, NF and neuronal nuclei, respectively. (C-c-1-c-4) Staining of N1 + GFAP, N1, GFAP and astrocyte nuclei, respectively. (D-d-1-d-4) Staining of N1 + GALC, N1, GALC and oligodendrocyte nuclei, respectively. Green indicates the positive staining of N1, Red indicates the positive staining of Nestin, NF, GFAP or GALC. Blue indicates Hoechst-labelled nuclei. Scale bar, 100 μM. N1, Notch1; PS1, presenilin 1; NF, neurofilament; GFAP, glial fibrillary acidic protein; GALC, galactocerebroside.

the bottom of the flask. Then, 1 day after differentiation, the size of neurospheres began to increase, and some NSCs were released from the neurospheres. Cells that had divided by one cell grew into a suspended growth state of nerve cloned spheres, in which numerous cells gathered together (Fig. 3B). After 3 days, different types of cells appear around the cloned sphere. The edge was observed as a jagged single-cell boundary, with extending cord-like projections and a strong three-dimensional shape (Fig. 3C). After 7 days, the spherical three-dimensional appearance gradually dissipated. The cells in the cloned sphere had a tendency to migrate outwards. The cloned sphere was completely attached and a different shape of the cells, including neurons, astrocytes and oligodendrocytes, was detected (Fig. 3D).

Co-expression of N1 with Nestin, NF, GFAP and GALC in NSCs as detected using co-immunofluorescence staining. To confirm the cell differentiation, a co-immunofluorescence staining technique was used. The results demonstrated there were positive co-expressions of N1 (green) with Nestin (red), NF (red), GFAP (red) and GLAC (red) in NSCs, neurons, astrocytes and oligodendrocytes, respectively (Fig. 4A-D).

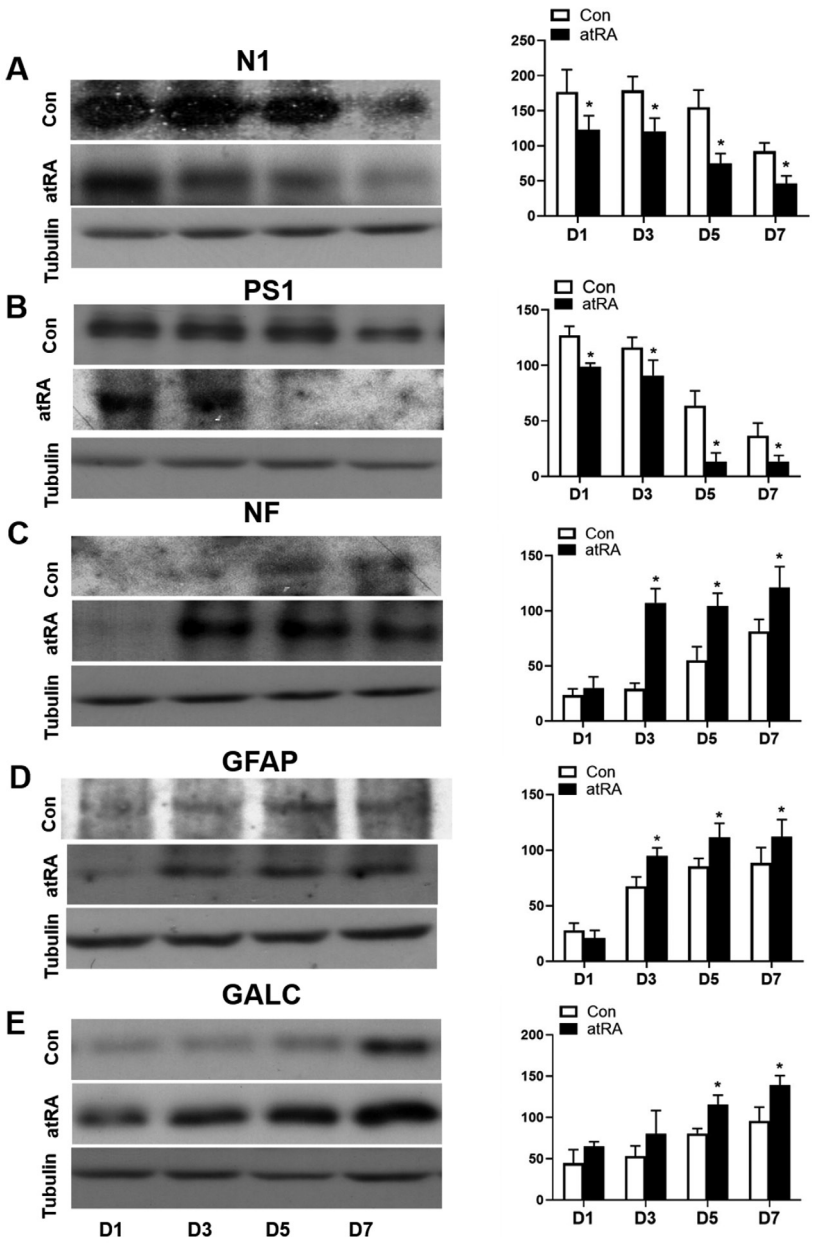

Figure 5. Expression levels of N1, PS1, NF, GFAP and GALC in neural cells at D1, 3, 5 and 7 treated with the Con or atRA media as detected by western blotting. Expression levels of (A) N1, (B) PS1, (C) NF, (D) GFAP and (E) GALC in atRA media have been compared with in control media. Tubulin was used as a control. *P<0.05 Con vs. atRA. Con, control media; N1, Notch1; PS1, presenilin 1; NF, meurofilament; GFAP, glial fibrillary acidic protein; GALC, galactocerebroside; atRA, all-*trans* retinoic acid; D, day.

Expression levels of N1, PS1, NF, GFAP and GALC in NSCs with or without atRA as detected via western blotting. Western blotting was performed to detect the expression levels of the proteins in NSCs. The results indicated that there were significantly decreased expression levels of N1 and PS1, but increased expression levels of NF, GFAP and GALC in NSCs from the atRA group compared with those in the controls (P<0.05; Fig. 5A-E). β-tubulin was used as a control. The results of statistical analyses have also been detailed in Table II.

Discussion

In vertebrates, NTDs originate from a failure in morphogenetic events that occur during the neurulation process (16). Nerve tubes and nerve sheaths are the origins of the nervous system. Nerve epithelial cells are NSCs that possess a variety of differentiation potentials during the development of nerve tubes (16). The normal proliferation and differentiation of NSCs is involved in the normal development of nerve tubes (17). Moreover, the development of the neural tube can be easily influenced by internal and external factors. For example, folic acid deficiency during pregnancy (18), use of antiepileptic drugs (19), exposure to heavy metals (20) and pesticides (21) all increase the risk of NTDs. Previous studies have reported that abnormal development of nerve epithelium is associated with NTDs, which occurs as the result of the differentiation of NSCs under various regulatory mechanisms, such as convergent extension, apical constriction, interkinetic nuclear migration and multiple signaling pathway (22). Furthermore, NSCs have the ability to self-renewal and diversify (23,24).

Table II. Data of N1, PS1, NF, GFAP and GALC expression levels in neural cells on days 1, 3, 5 and 7 with the control media (-atRA) or atRA media (+atRA) from western blotting.

		Control			+atRA			
Protein	Day	Exp.1	Exp.2	Exp.3	Exp.1	Exp.2	Exp.3	P-value
N1	D1	211.30	169.90	148.70	123.40	102.30	142.60	0.019
	D3	197.50	181.20	158.10	100.20	123.30	137.90	0.011
	D5	132.20	181.10	151.30	73.40	61.70	89.50	0.0007
	D7	79.80	93.60	103.30	36.70	58.40	42.50	0.048
PS1	D1	126.30	135.70	119.80	96.40	102.70	97.50	0.011
	D3	125.10	116.70	106.20	76.60	104.60	91.30	0.025
	D5	59.90	78.50	52.40	21.30	5.10	12.70	<0.0001
	D7	37.60	47.40	24.30	12.30	19.20	8.30	0.042
NF	D1	18.30	22.40	29.60	32.50	18.90	38.60	0.94
	D3	33.10	31.10	23.50	103.30	121.60	96.70	<0.0001
	D5	51.60	44.80	68.70	93.50	103.60	116.30	0.0004
	D7	71.30	93.20	78.80	123.70	138.50	101.20	0.0027
GFAP	D1	21.10	28.90	33.80	15.40	18.70	28.60	0.88
	D3	67.80	75.70	58.90	102.30	88.20	94.30	0.018
	D5	92.50	78.10	85.30	98.90	112.30	123.70	0.024
	D7	82.70	78.30	104.20	109.50	128.60	98.60	0.045
GALC	D1	62.70	39.80	31.30	59.70	70.80	64.20	0.40
	D3	61.80	38.70	58.50	49.60	104.60	86.70	0.16
	D5	73.60	81.80	85.60	126.40	116.70	103.80	0.044
	D7	113.50	92.70	79.80	148.90	126.60	142.10	0.010

Control, without all-*trans* retinoic acid; +atRA, with all-*trans* retinoic acid; D, experiment day; Exp., experiment; N1, Notch1; PS1, presenilin 1; NF, neurofilament; GFAP, glial fibrillary acidic protein; GALC, galactocerebroside.

atRA is a powerful inducer that can cause NTDs. Previous studies have revealed that atRA-induced NTDs are associated with the abnormal expression of Smad protein (25,26). atRA induces significant alterations in the expression of various stemness and differentiation genes associated with neuro-glial differentiation in NSCs (22). However, there is little research on the effect of atRA on the proliferation and differentiation of NSCs. Therefore, the primary focus of the present study was to investigate the effect of atRA on N1 expression in NSCs to identify the teratogenic mechanism of atRA.

The Notch signaling pathway influences the development of multiple biological functions, including differentiation, proliferation and apoptosis (27). Notch signaling has previously been reported to be inhibited during atRA-induced glioblastoma stem cell growth inhibition (28). In the present study, the effects of atRA on primary neurulations were investigated during neurogenesis. It was identified that N1 expression was downregulated in atRA-treated E11-17 embryos compared with that in the controls. The present results indicated that atRA promoted neural tube differentiation via the suppression of N1 activation.

To further investigate the effects of N1 in atRA-induced stem cells fate, primary NSCs were extracted from the fetal brain of 18.5-day pregnant mice. After differentiation of the culture medium to cultivate NSCs, cells could be divided into neurons, astrocytes and oligodendrocytes, as indicated via morphology and immunofluorescence identification. It was demonstrated that NSCs had self-renewal and multidirectional differentiation capabilities, which was consistent with previous studies (29,30). Moreover, the expression of N1 on the cell membrane and cytoplasm of differentiated neurons, astrocytes and oligodendrocytes was detected via co-immunofluorescence, and it was suggested that N1 was associated with the differentiation of NSCs.

The Notch signal pathway serves a regulatory role in cell proliferation and differentiation (8). The ubiquitination of PS1 by *C. elegans* SEL-10 targets PS1 for degradation via the ubiquitin-proteasome system and antagonizes the activity of the Notch signaling pathway (31). Previous studies have reported that PS1, the main factor of the presenilin γ-secretase enzymes, activates the downstream molecules of the Notch signaling pathway (31-33). In accordance with the present results of the *in vivo* study, N1 expression was downregulated in atRA-treated NSCs. Furthermore, the expression of PS1, as the target of atRA in Notch signaling, was detected. The results demonstrated that the PS1 was also downregulated in atRA-treated NSCs.

Based on the present results, western blotting was conducted to further detect the expression levels of N1 and PS1 and the differentiation of NSCs with or without atRA.

In untreated NSCs, the expression levels of both N1 and PS1 were regularly decreased, but there were significant increases in NF, GALC and GFAP expression levels in a time-dependent manner. It was suggested that the decreased expression levels of N1 and PS1 were synchronous, and when the expression of both of these factors declined the markers of neurons, astrocytes and oligodendrocytes, including NF, GALC and GFAP, were significantly increased. Moreover, it was indicated that the decrease of N1 expression, to a certain degree, significantly promoted the differentiation of NSCs. After the treatment of NSCs with atRA, the expression levels of N1 and PS1 gradually decreased, but the expression levels of NF, GALC and GFAP were increased significantly. Thus, the present results demonstrated that after atRA treatment, the differentiation ability of NSCs was increased.

In NTDs, the role of Notch1 signaling pathway is complex. Recent research has revealed the inhibition of N1 by suppressing the RhoA/ROCK1 signaling pathway caused a decreased in the expression levels of its target genes, hes family bHLH transcription factor 1 (Hes1) and Hes5, which led to the promotion of neuronal differentiation (34). To the best of our knowledge, the present study provided the first evidence that N1 inhibits NSC differentiation via the activation of PS1. After NSCs were treated with atRA, the expression of N1 was gradually decreased via the inhibition of PS1, and the markers of the differentiated cells, such as neurons, astrocytes and oligodendrocytes, were significantly increased, indicating that atRA promoted the differentiation of NSCs by inhibiting PS1. However, the present study has some limitations. For example, the changes of N1 expression were studied only at the protein level, and the downstream factors associated with the Notch pathways were not further investigated. Thus, future studies will examine the relationship between the target genes Hes1 and Hes5 and the N1 signaling pathway in NTDs at the gene and protein levels.

Collectively, the present results provided evidence to improve the understanding of the molecular mechanism of NTDs, such as brain bulging, meningeal membrane bulging and recessive spinal bifida, which are caused by increased amounts of atRA. The present study demonstrated the role of atRA in the successful development of the neural tube, as well as identified the common etiology for a spectrum of idiopathic anomalies that characterize certain human congenital disorders. These findings highlighted the molecular and teratogenic actions of atRA and may contribute to the development of potential novel treatments for NTDs in the future.

In conclusion, the present study demonstrated that atRA mainly promoted the differentiation of NSCs by inhibiting the action of γ-secretase enzymes, which activated the Notch signal pathway. These conclusions provide not only a theoretical basis for the future clinical application of NSCs, but also a novel treatment window for the prevention of fetal NTDs.

Acknowledgements

Not applicable.

Funding

The present study was supported by the Shandong Natural Foundation, China (grant no. ZR2017MH021), the National Natural Science Foundation (grant no. 81400166) and the Key Research and Development Program of Shandong Province (grant no. 2018GSF118157).

Availability of data and materials

All data generated or analyzed during the present study are included in this published article.

Authors' contributions

NC, BH and AM designed the study and edited the manuscript. JX, SL, HC and XZ performed the experiments. WZ and YS analyzed the data. All authors read and approved the manuscript.

Ethics approval and consent to participate

All the experiments complied with the guidance by the Animal Use and Care of Shandong Provincial Hospital Affiliated to Shandong First Medical University and the agents were approved by the Ethical Committee of Animal Care and Use. The research was approved by the Medical Ethics Committee of Shandong Provincial Hospital Affiliated to Shandong First Medical University.

Patient consent for publication

Not applicable.

Competing interests

The authors declare that they have no competing interests.

References

1. Zaganjor I, Sekkarie A, Tsang BL, Williams J, Razzaghi H, Mulinare J, Sniezek JE, Cannon MJ and Rosenthal J: Describing the Prevalence of Neural Tube Defects Worldwide: A Systematic Literature Review. PLoS One 11: e0151586, 2016.
2. Copp AJ and Greene ND: Neural tube defects - disorders of neurulation and related embryonic processes. Wiley Interdiscip Rev Dev Biol 2: 213-227, 2013.
3. Copp AJ, Stanier P and Greene ND: Neural tube defects: Recent advances, unsolved questions, and controversies. Lancet Neurol 12: 799-810, 2013.
4. Lowery LA and Sive H: Strategies of vertebrate neurulation and a re-evaluation of teleost neural tube formation. Mech Dev 121: 1189-1197, 2004.
5. Nikolopoulou E, Galea GL, Rolo A, Greene ND and Copp AJ: Neural tube closure: cellular, molecular and biomechanical mechanisms. Development 144: 552–566, 2017.
6. Liang S, Yin N and Faiola F: Human Pluripotent Stem Cells as Tools for Predicting Developmental Neural Toxicity of Chemicals: Strategies, Applications, and Challenges. Stem Cells Dev 28: 755-768, 2019.
7. Daadi MM: Generation of Neural Stem Cells from Induced Pluripotent Stem Cells. Methods Mol Biol 1919: 1-7, 2019.
8. Artavanis-Tsakonas S, Rand MD and Lake RJ: Notch signaling: Cell fate control and signal integration in development. Science 284: 770-776, 1999.
9. Andersson ER, Sandberg R and Lendahl U: Notch signaling: Simplicity in design, versatility in function. Development 138: 3593-3612, 2011.
10. Bray SJ: Notch signalling in context. Nat Rev Mol Cell Biol 17: 722-735, 2016.
11. Ni X, Hu G and Cai X: The success and the challenge of all-*trans* retinoci acid in the treatment of cancer. Crit Rev Food Sci Nutr 59 (Suppl. 1): S71- S80, 2019.

12. Sewell W and Kusumi K: Genetic analysis of molecular oscillators in mammalian somitogenesis: Clues for studies of human vertebral disorders. Birth Defects Res C Embryo Today 81: 111-120, 2007.
13. Liu D, Xue J, Liu Y, Gu H, Wei X, Ma W, Luo W, Ma L, Jia S, Dong N, *et al*: Inhibition of NRF2 signaling and increased reactive oxygen species during embryogenesis in a rat model of retinoic acid-induced neural tube defects. Neurotoxicology 69: 84-92, 2018.
14. Seegmiller RE, Ford WH, Carter MW, Mitala JJ and Powers WJ Jr: A developmental toxicity study of tretinoin administered topically and orally to pregnant Wistar rats. J Am Acad Dermatol 36: S60-S66, 1997.
15. El Hajj A, Yen FT, Oster T, Malaplate C, Pauron L, Corbier C, Lanhers MC and Claudepierre T: Age-related changes in regio-specific expression of Lipolysis Stimulated Receptor (LSR) in mice brain. PLoS One 14: e0218812, 2019.
16. Cearns MD, Escuin S, Alexandre P, Greene ND and Copp AJ: Microtubules, polarity and vertebrate neural tube morphogenesis. J Anat 229: 63-74, 2016.
17. McShane SG, Molè MA, Savery D, Greene ND, Tam PP and Copp AJ: Cellular basis of neuroepithelial bending during mouse spinal neural tube closure. Dev Biol 404: 113-124, 2015.
18. Leung KY, Pai YJ, Chen Q, Santos C, Calvani E, Sudiwala S, Savery D, Ralser M, Gross SS, Copp AJ, *et al*: Partitioning of one-carbon units in folate and methionine metabolism is essential for neural tube closure. Cell Rep 21: 1795-1808, 2017.
19. Nau H, Hauck RS and Ehlers K: Valproic acid-induced neural tube defects in mouse and human: Aspects of chirality, alternative drug development, pharmacokinetics and possible mechanisms. Pharmacol Toxicol 69: 310-321, 1991.
20. Jin L, Zhang L, Li Z, Liu JM, Ye R and Ren A: Placental concentrations of mercury, lead, cadmium, and arsenic and the risk of neural tube defects in a Chinese population. Reprod Toxicol 35: 25-31, 2013.
21. Ren A, Qiu X, Jin L, Ma J, Li Z, Zhang L, Zhu H, Finnell RH and Zhu T: Association of selected persistent organic pollutants in the placenta with the risk of neural tube defects. Proc Natl Acad Sci USA 108: 12770-12775, 2011.
22. Kanakasabai S, Pestereva E, Chearwae W, Gupta SK, Ansari S and Bright JJ: PPARγ agonists promote oligodendrocyte differentiation of neural stem cells by modulating stemness and differentiation genes. PLoS One 7: e50500, 2012.
23. Mohlin S, Kunttas E, Persson CU, Abdel-Haq R, Castillo A, Murko C, Bronner ME and Kerosuo L: Maintaining multipotent trunk neural crest stem cells as self-renewing crestospheres. Dev Biol 447: 137-146, 2019.
24. Urata Y, Yamashita W, Inoue T and Agata K: Spatio-temporal neural stem cell behavior leads to both perfect and imperfect structural brain regeneration in adult newts. Biol Open 7: bio033142, 2018.
25. Zhang J, Li R, He Q, Li WI, Niu B, Cheng N, Zhou R, Zhang T, Zheng X and Xie J: All-*trans*-retinoic acid alters Smads expression in embryonic neural tissue of mice. J Appl Toxicol 29: 364-366, 2009.
26. Lee SH, Shin JH, Shin MH, Kim YS, Chung KS, Song JH, Kim SY, Kim EY, Jung JY, Kang YA, *et al*: The effects of retinoic acid and MAPK inhibitors on phosphorylation of Smad2/3 induced by transforming growth factor β1. Tuberc Respir Dis (Seoul) 82: 42-52, 2019.
27. Ryu HW, Park CW and Ryu KY: Disruption of polyubiquitin gene Ubb causes dysregulation of neural stem cell differentiation with premature gliogenesis. Sci Rep 4: 7026, 2014.
28. Ying M, Wang S, Sang Y, Sun P, Lal B, Goodwin CR, Guerrero-Cazares H, Quinones-Hinojosa A, Laterra J and Xia S: Regulation of glioblastoma stem cells by retinoic acid: Role for Notch pathway inhibition. Oncogene 30: 3454-3467, 2011.
29. De Filippis L, Zalfa C and Ferrari D: Neural Stem Cells and Human Induced Pluripotent Stem Cells to Model Rare CNS Diseases. CNS Neurol Disord Drug Targets 16: 915-926, 2017.
30. Dunnett SB and Rosser AE: Cell transplantation for Huntington's disease Should we continue? Brain Res Bull 72: 132-147, 2007.
31. Li J, Pauley AM, Myers RL, Shuang R, Brashler JR, Yan R, Buhl AE, Ruble C and Gurney ME: SEL-10 interacts with presenilin 1, facilitates its ubiquitination, and alters A-beta peptide production. J Neurochem 82: 1540-1548, 2002.
32. Duggan SP and McCarthy JV: Beyond γ-secretase activity: The multifunctional nature of presenilins in cell signalling pathways. Cell Signal 28: 1-11, 2016.
33. De Strooper B, Annaert W, Cupers P, Saftig P, Craessaerts K, Mumm JS, Schroeter EH, Schrijvers V, Wolfe MS, Ray WJ, *et al*: A presenilin-1-dependent gamma-secretase-like protease mediates release of Notch intracellular domain. Nature 398: 518-522, 1999.
34. Peng Z, Li X, Fu M, Zhu K, Long L, Zhao X, Chen Q, Deng DYB and Wan Y: Inhibition of Notch1 signaling promotes neuronal differentiation and improves functional recovery in spinal cord injury through suppressing the activation of Ras homolog family member A. J Neurochem 150: 709-722, 2019.